THE JOURNAL OF PHYSICAL CHEMISTRY B

Article

pubs.acs.org/JPCB

RGDC Functionalized Titanium Dioxide Nanoparticles Induce Less Damage to Plasmid DNA but Higher Cytotoxicity to HeLa Cells

Yuan Yin,[†] Wei-Wei Zhu,[‡] Li-Ping Guo,[‡] Ran Yang,[†] Xin-Song Li,[†] and Yong Jiang*,[†]

[†]School of Chemistry and Chemical Engineering and [‡]School of Materials Science and Engineering, Southeast University, Jiangning, Nanjing, Jiangsu, 211189, People's Republic of China

Supporting Information

ABSTRACT: In this paper, nano-TiO_2 was functionalized by different methods, and its genotoxicity and cytotoxicity were studied in detail. The genotoxicity of nano-TiO_2 was evaluated by observing its interactions with pUC19 plasmid DNA at a single molecule level using atomic force microscopy. The results show that with the assistance of UVA radiation, RGDC functionalized nano-TiO_2 induced less damage to plasmid DNA than unmodified ones. The HeLa cell-specific PDT effect was investigated by cytotoxicity assay correspondingly. RGDC-functionalized nano-TiO_2 shows the highest killing effect to HeLa cells with the assistance of UVA radiation. The reasons that cause the contradiction between genotoxicity and cytotoxicity were analyzed, and the molecular mechanisms of the PDT effects were discussed. The results show that the genotoxicity of nano-TiO_2 to plasmid DNA and its cytotoxicity to HeLa cells are related but also different. The RGDC functionalization is an effective method to increase the cytotoxicity of nano-TiO_2.

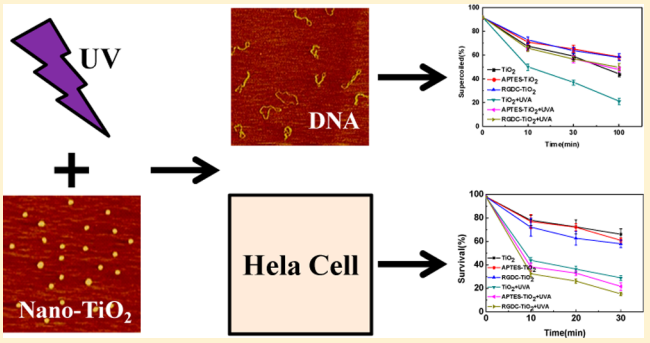

INTRODUCTION

Nanomedicine is the application of nanomaterials and nanotechnology to medicine, which enables the development of nanoparticles as the therapeutic media.[1,2] Some of the nanomaterials are targetable carriers for chemical drugs, while some of them can work as the therapeutics themselves with the assistance of light or ultrasonic waves. Titanium dioxide nanoparticles (nano-TiO_2) are one of the most attractive engineered nanomaterials for use in many fields.[3,4] Nano-TiO_2 can be activated by ultraviolet (UV) light because its energy is greater than the band gap of nano-TiO_2 (~3.0 eV).[5] The activated nano-TiO_2 is capable of undergoing electron transfer reactions, followed by photogenerated electron holes.[6] This activation results in the immediate production of superoxide anions (O_2^-) that convert to multiple reactive oxygen species (ROS), including hydrogen peroxide (H_2O_2), hydroxyl radicals (OH^-), and peroxynitrites.[7,8]

Because of the photocatalytic effects of nano-TiO_2, many recent studies indicate that nano-TiO_2 could be nanotoxic to biological targets that are sensitive to oxidative stress damage. In aqueous solution, the ROS produced by nano-TiO_2 can lead to the cleavage of DNA strands[9−11] and induce the formation of oxidative damage to DNA.[12−14] Moreover, nano-TiO_2 and its photocatalytic products can react with proteins and decrease their activities.[15,16] Furthermore, the nanotoxicities of TiO_2 to brain cells[4] and liver injury[17] were also reported.

The above research has demonstrated that nano-TiO_2 have distinct genotoxicity and cytotoxicity. If we can modify the surface of TiO_2 and make it targetable to the cancer cell, it could be a very good candidate for therapeutic tumor treatment. In recent years, nano-TiO_2 has been viewed as a potential photosensitizing agent for photodynamic therapy (PDT) of malignant cells.[2,18,19] Some researchers showed that the ROS produced by nano-TiO_2 could be applied to kill cancer cells.[19−23] Moreover, it was reported that the surface of nano-TiO_2 was modified with antibodies to recognize cancer cells to localize the ROS effect toward the targeted cells.[24,25] One important issue needed to be stated here is that the genotoxicity and cytotoxicity of nano-TiO_2 take effect only if UV light is applied, so it provides a switch to control the activation of the therapeutic function. In the most recent work, this therapeutic effect can even be activated by visible light irradiation[26−30] or sonodynamic therapy (SDT).[18,31] However, few papers were reported on the therapeutic effects of RGDC-functionalized nano-TiO_2, and the relationship between therapeutic effects and DNA damage is still unknown.

In the present work, we address the PDT effects of nano-TiO_2 functionalized by RGDC peptide to HeLa cells. By cytotoxicity assays, the cancer cell specific photokilling effects of functionalized nano-TiO_2 were evaluated with the assistance of UVA irradiation. Furthermore, the molecular mechanisms of PDT effects were studied using atomic force microscopy

Received: September 18, 2012
Revised: November 15, 2012
Published: December 4, 2012

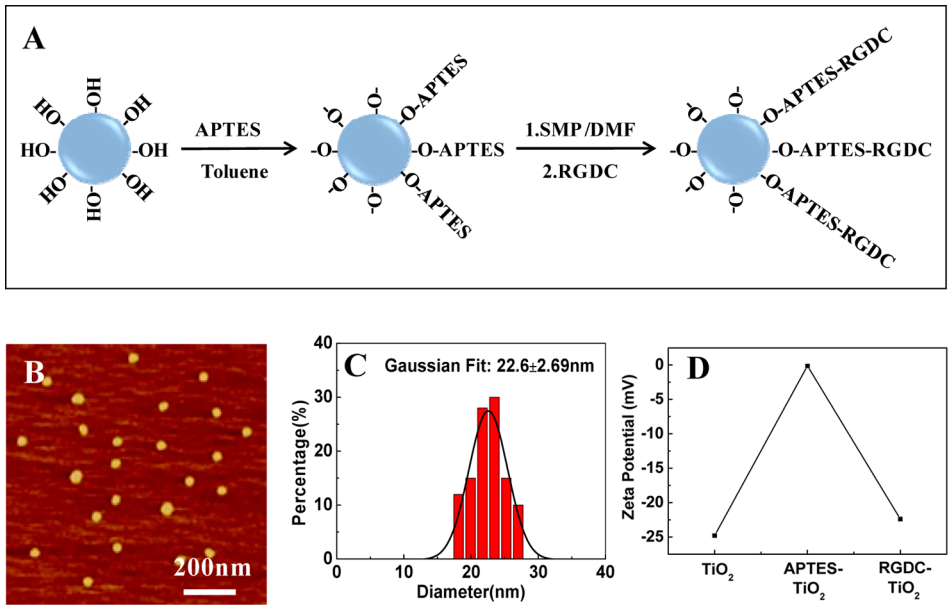

Figure 1. (A) Sketch map demonstrates the functionalization process of nano-TiO_2. (B) AFM height image shows the unmodified nano-TiO_2 particles on a mica surface, and the scan size is 1000 nm. (C) Histogram summarizes the distribution of diameters of nano-TiO_2 that were determined from the AFM images, such as the image shown in panel B. (D) ζ-Potentials of three different kinds of nano-TiO_2 particles at a pH value of 8.0.

(AFM) at a single molecule level. The relationship between the cytotoxicity and the genotoxicity is discussed in detail. To the best of our knowledge, our paper shows the first direct images of the interaction of nano-TiO_2 on a single DNA molecule captured by AFM.

EXPERIMENTAL METHODS

Materials. PUC19 plasmid DNA substrate (2686 base pairs) was purchased from New England Biolabs. Titanium dioxide (anatase crystal with the size less than 25 nm) was bought from Sigma-Aldrich. Both Tris-EDTA buffer (100× concentrated with 1.0 M Tris-HCl and 0.1 M EDTA, pH 8.0) and 3-aminopropyltriethoxysilane (APTES) were also ordered from Sigma-Aldrich. Peptide Arg−Gly−Asp−Cys (RGDC) and *n*-succinimidyl-3-maleimidopropionate (SMP) were purchased from Chutai BioTech Company in Shanghai, China (http://www.apeptide.com). *N*,*N*-Dimethylformamide (DMF) was obtained from Sinopharm Chemical Reagent Beijing Co., Ltd. (www.crc-bj.com). Fetal bovine serum (FBS), Dulbecco's modified Eagle's medium (DMEM), and 3-(4,5-dimethylthiazol-2-yl)-2,5-diphenyltetrazolium bromide (MTT) were purchased from Gibco Life Technologies.

Functionalization of Nano-TiO_2. Nano-TiO_2 was functionalized with APTES and RGDC peptide according to previous reports.[32] Prior to silanization, nano-TiO_2 was incubated in a solution of 1:1 (v/v) methanol/HCl (37%) for 30 min and rinsed with deionized water. Then, it was treated with sulfuric acid (98%) for 15 min, washed extensively with deionized water and acetone, and dried under vacuum for 12 h. Silanization was performed by incubating nano-TiO_2 at 120 °C for 3 h in 30 mL of dry toluene containing 1.2 mL (2.15 mM) of APTES. After that, silanized nano-TiO_2 (APTES-TiO_2) was ultrasonically washed with chloroform, acetone, methanol, and deionized water. APTES-TiO_2 was incubated in 1.2 mL of DMF containing 9 mg of SMP (28 mM) for 1 h. The SMP-functionalized nano-TiO_2 (SMP-TiO_2) was washed with DMF and water. To prevent hydrolysis, the substrates were immediately subjected to the next reaction step. The SMP-TiO_2 was incubated in 1.2 mL of pure water containing 5.4 mg of RGDC (10 mM) for 2 h. The pH value of the solution was adjusted to 7.0 with 0.1 M NaOH because of the presence of CF_3COOH in the peptide solutions. The final product RGDC functionalized TiO_2 (RGDC-TiO_2) was washed thoroughly with deionized water, dried by nitrogen, and stored in argon for future use.

ζ-Potential. The ζ-potentials of TiO_2, APTES-TiO_2, and RGDC-TiO_2 were measured by the Zetasizer Nano Analyzer (Malvern Instruments Inc.) at a temperature of 25 °C and a pH value of 8.0.

Treatment of DNA with Different Nano-TiO_2 and UVA Irradiation. PUC19 DNA at a concentration of 0.5−1.0 μg/mL was incubated with nano-TiO_2 (10.0 μg/mL) in reaction buffer (10 mM Tris HCl, 1 mM EDTA, 100 mM NaCl, and 10 mM $MgCl_2$) at room temperature for different times (10, 30, and 100 min). For some of the experiments, UVA irradiation was applied at a wavelength of 365 nm during the incubation using a multiwavelength UV lamp (6W) from Nanjing Keer Instrument Equipment Co., Ltd.

AFM Imaging. Fresh mica was used for the binding of DNA molecules. A drop of 30−50 μL of DNA solution (0.5−1 μg/mL) was deposited on the mica surface for 3 min at room temperature. The sample was rinsed and air-dried before imaging. Images were taken in air at room temperature by a Dimension Icon Scanning Probe Microscope with Nanoscope V Controller (Bruker Instruments) using Tapping Mode. RTESP probes (Bruker Instruments) were used for imaging in air. The spring constant of AFM cantilevers was 20−80 N/m, and their resonance frequency was 275−316 kHz. All images were collected at a scan rate of 2.0−3.0 Hz, a scan line of 512 × 512 pixels, and scan sizes of 1000−5000 nm. In each experiment, more than 15 AFM images were captured and analyzed to determine the fractions of supercoiled, relaxed circular, and linear molecules. The results are expressed as the mean ± SD for each fraction.

dx.doi.org/10.1021/jp3092804 | J. Phys. Chem. B 2013, 117, 125−131

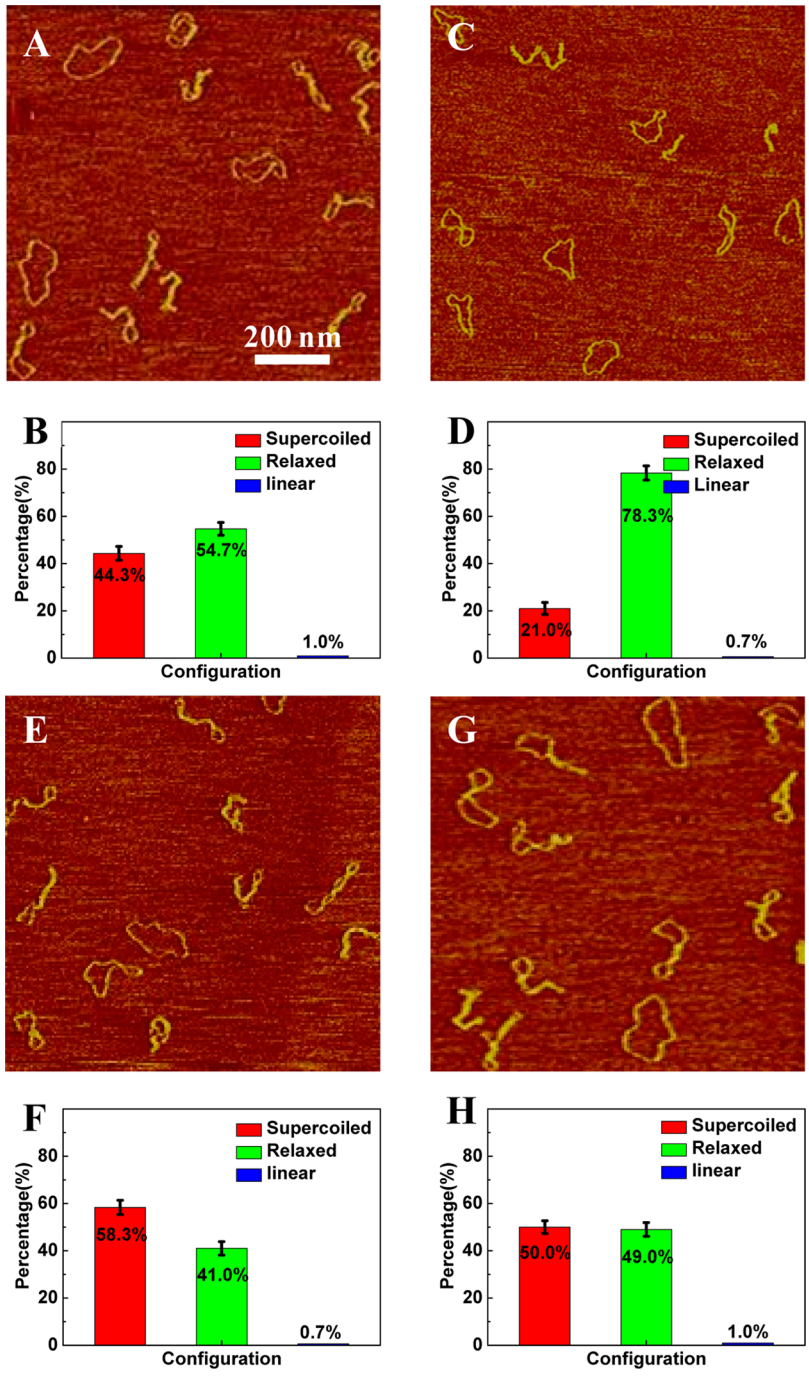

Figure 2. (A, C, E, and G) AFM height images of supercoiled pUC19 DNAs (0.5−1.0 μg/mL) after incubation with nano-TiO_2 (10.0 μg/mL) in reaction buffer (10 mM Tris HCl, 1 mM EDTA, 100 mM NaCl, and 10 mM $MgCl_2 \cdot 6H_2O$) for 100 min. Supercoiled pUC19 DNA was interacted with unmodified nano-TiO_2 in the absence (A and B) and presence (C and D) of UVA radiation. Supercoiled pUC19 DNA was interacted with RGDC-TiO_2 in the absence (E and F) and presence (G and H) of UVA radiation. After the incubation, the solution was used for AFM imaging directly. The scan size in all AFM images is 1000 nm. Among them, B, D, F, and H are histograms of the occurrence of various configurations of pUC19 plasmids determined from the corresponding AFM images. Color code: red, supercoiled DNA; green, relaxed circular plasmids; and blue, linear DNA. The error bars in the figures represent the standard deviation. Each histogram is based on about 300 DNA molecules from more than 15 AFM images.

Cytotoxicity Assays. The cytotoxicity of nano-TiO_2 was measured by MTT assay using a human cervical cancer cell line (HeLa cells).[33] HeLa cells were seeded at the density of approximately 10^4 cells/well in 96-well plates and grown in 100 μL of DMEM medium containing 10% FBS for 12 h at 37 °C. The cells were incubated with 100 μL of different concentrations (10, 100, and 1000 μg/mL) of nano-TiO_2, APTES-TiO_2, and RGDC-TiO_2 for different times (10, 20, and 30 min). For some of the experiments, UVA radiation was applied using a multiwavelength UV lamp (20W) from Nanjing Keer Instrument Equipment Co., Ltd. After the cells were treated with nano-TiO_2, the medium was replaced with DMEM containing 10% FBS, and 20 μL of MTT solution (5 mg/mL in PBS) was added, and the cells were further incubated for 4 h at

dx.doi.org/10.1021/jp3092804 | J. Phys. Chem. B 2013, 117, 125−131

37 °C. Subsequently, the medium was removed carefully, and 150 μL of DMSO was added to each well to dissolve the formazan crystal formed by proliferating cells. The cells were also incubated for 4 h in the same medium supplemented with 10% serum. The volume was adjusted to have the same number of nanoparticles per cell in all culture conditions. The absorbance was measured at 490 nm using a microplate reader (model 680, Bio-Rad, United States). The cell viability was calculated as a percentage of complex-treated cells to untreated negative control cells.

RESULTS AND DISCUSSION

Functionalization of Nano-TiO_2. Figure 1A is a sketch map showing the functionalization process of nano-TiO_2. Figure 1B is an AFM image showing the appearances of unmodified nano-TiO_2. All of the TiO_2 nanoparticles were quite uniform with similar shapes and sizes. The diameters of these nanoparticles were measured by AFM software, and the distribution of the diameters is shown in Figure 1C. On the basis of the Gaussian fit of the distribution, the average size of TiO_2 nanoparticles was 22.6 ± 2.7 nm (mean ± standard deviation), which is consistent with the description by the vender. Surface ζ-potentials of the functionalized nanoparticles obtained at different stages were measured to monitor the reaction process. The ζ-potentials for unmodified nano-TiO_2 are measured to be −24.8 mV at a pH value of 8.0, which is consistent with the results obtained by other researchers.[34] The ζ-potentials of APTES-TiO_2 and RGDC-TiO_2 are −0.1 and −22.4 mV, respectively, which implied that the functionalization processes were successful. The morphologies of functionalized nano-TiO_2 were also measured by AFM (data are not shown here), and no clear differences in terms of appearance and size were observed between the functionalized TiO_2 and the unmodified ones.

Genotoxicity of Three Kinds of Nano-TiO_2. Native pUC19 plasmid with supercoiled structure was chosen as a DNA substrate to detect DNA damage by nano-TiO_2. The configuration of pUC19 DNA is highly sensitive to its structural modifications; that is, one single strand break (SSB) will convert its structure to relaxed circular form, and one double strand break (DSB) will turn the circular DNA into a linear structure, and the changes in structures can be easily identified by AFM imaging.[35,36] As we presented in the Introduction, ROS generated by nano-TiO_2 can induce SSB and DSB to DNA stands, so DNA damage caused by nano-TiO_2 can be resolved simply by visualizing individual intact and damaged plasmids in AFM. Besides, nano-TiO_2 may also produce base modifications such as oxidative lesions on DNA bases. Because these base lesions could not cause clear changes to the structure of DNA, they are not able to be observed directly by AFM imaging. In this case, appropriate endonuclease (e.g., *Escherichia coli* Fpg Glycosylase is able to cleave the DNA strands at 8-oxoguanine sites) can be adapted to convert those base lesions into SSBs.

Figure 2A is the AFM image that shows the pUC19 plasmid DNA after interacting with unmodified nano-TiO_2 for 100 min, and no UVA radiation was applied during the interaction. The numbers of supercoiled and relaxed circular DNA were counted based on this image and similar images. The statistical result (Figure 2B) shows that less than 44 ± 3% of DNA was found to remain in supercoiled form, while more than 55 ± 3% of DNA became relaxed, which means 55 ± 3% of DNA had at least one SSB among the plasmid stands. Supporting Figure S1A in the Supporting Information is an AFM image showing the intact pUC19 plasmid DNA deposited on the mica from a buffer solution. All of the DNA molecules shown in this image kept the plectonemic supercoiled configuration. Neither the binding to the mica nor the AFM imaging process affected the DNA structure. The statistical results showed that 92 ± 3% of DNA was supercoiled (Supporting Figure S1B in the Supporting Information). Furthermore, when UVA radiation was applied during the similar interaction process of DNA and nano-TiO_2 as above, more supercoiled DNA was observed to be in the relaxed form (Figure 2C) and the percentage of supercoiled DNA decreased from 44 ± 3 to 21 ± 3%, while the percentage of relaxed DNA increased from 55 ± 3 to 78 ± 3% (Figure 2D). On the basis of our control results (data not shown) and former research,[36] UVA radiation at this dose could not cause clear SSB and DSB to DNA molecules directly. It means that when UVA radiation was applied, the additional damage was produced by UVA-activated nano-TiO_2 not by UVA radiation itself directly.

Similar interactions between pUC19 DNA and functionalized TiO_2 were performed using APTES-TiO_2 (Figure 3) and

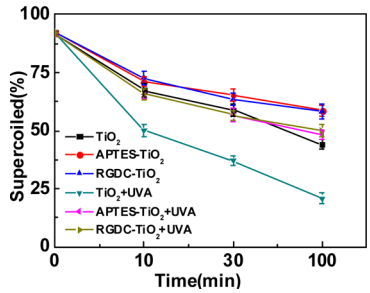

Figure 3. Curves summarized the percentages of supercoiled pUC19 plasmid DNA after incubation with nano-TiO_2 as a function of time. Supercoiled pUC19 DNA (0.5−1.0 μg/mL) was incubated with three different kinds of nano-TiO_2 (10.0 μg/mL) with or without the assistance of UVA radiation as shown in Figure 2 in the reaction buffer (10 mM Tris HCl, 1 mM EDTA, 100 mM NaCl, and 10 mM $MgCl_2 \cdot 6H_2O$) for different times (10, 30, and 100 min).

RGDC-TiO_2 (Figures 2E−H and 3). When RGDC-TiO_2 was used to interact with pUC19 in the same experimental condition as used in Figure 2A, 58 ± 3% of DNA remained undamaged supercoiled, and relaxed DNA took the ratio of 41 ± 2% (Figure 2E,F). When UVA radiation was applied during the incubation, the percentages of supercoiled and relaxed circular DNA were 50 ± 3 and 49 ± 3%, respectively.

The interactions between pUC19 plasmid DNA and three kinds of nano-TiO_2 were performed in detail at different incubation times (10, 30, and 100 min), and the results are summarized in Figure 3. First, for all three kinds of nano-TiO_2, the percentages of supercoiled DNA went down as the incubation time increased. Second, for each kind of nano-TiO_2, more damage was detected with the assistance of UVA radiation than the ones without UVA radiation. Third, in the same experimental condition, unmodified nano-TiO_2 generated more damage than functionalized nano-TiO_2. So, as a summary, with the assistance of UVA radiation, RGDC-functionalized nano-TiO_2 induced less damage to plasmid DNA than unmodified ones.

Cytotoxicity of Three Kinds of Nano-TiO_2. The cytotoxicities of three kinds of nano-TiO_2 (with and without UVA irradiation) were determined by exposing HeLa cells to

dx.doi.org/10.1021/jp3092804 | J. Phys. Chem. B 2013, 117, 125−131

these nano-TiO_2 for different times (10, 20, and 30 min as shown in Figure 4) at various concentrations (10, 100, and

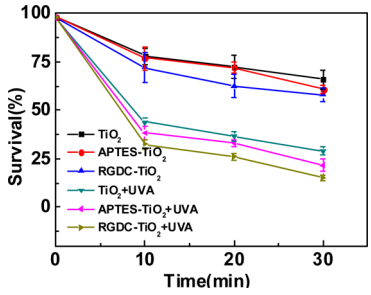

Figure 4. Curves summarized the percentages of survivals of HeLa cells after interaction with nano-TiO_2 as a function of time. HeLa cells (about 10^2 cells/μL) were incubated with three different kinds of nano-TiO_2 (1000 μg/mL) in the absence and presence of UVA radiation for different times (10, 20, and 30 min).

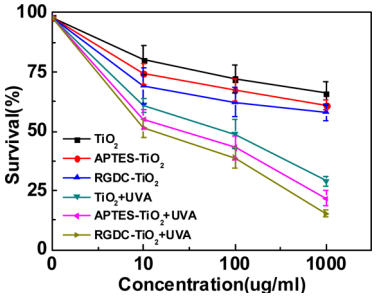

Figure 5. Curves summarized the percentages of survivals of HeLa cells after interaction with nano-TiO_2 as a function of the concentration of nano-TiO_2. HeLa cells (about 10^2 cells/μL) were incubated with three kinds of nano-TiO_2 at different concentrations (10, 100, and 1000 μg/mL) in the absence and presence of UVA radiation for 30 min.

1000 μg/mL as shown in Figure 5). As shown by the black curve in Figure 4, the surviving fraction of HeLa cells is given as a function of the irradiation time of UVA. When HeLa cells were treated with unmodified nano-TiO_2 (1000 μg/mL) in the absence of UVA radiation, the survival was 78 ± 4% after 10 min of incubation. It means about 22% of cells were killed after 10 min of exposure, which indicates that unmodified nano-TiO_2 alone without UVA irradiation showed small toxicity to HeLa cells. Whereas after 30 min of exposure, about 66 ± 5% of the cells remained alive, and 34% of them were killed.

Comparing the cytotoxicity results of APTES-TiO_2 (red curve) and RGDC-TiO_2 (blue curve) with unmodified nano-TiO_2 (black curve), it is clear that both functionalized nano-TiO_2 particles show higher cytotoxicity to HeLa cells than unmodified nano-TiO_2. After 10 min of incubation with functionalized nano-TiO_2, the survival rates were 77 ± 6 and 72 ± 7% for APTES-TiO_2 and RGDC-TiO_2 respectively, and for 30 min of incubation, the survival rates decreased to 61 ± 2 and 58 ± 3%, respectively.

With the assistance of UVA irradiation, the HeLa cells were killed by nano-TiO_2 at a much higher rate (Figure 4). In the presence of 1000 μg/mL of unmodified TiO_2 (dark cyan curve in Figure 4), 44 ± 2% of the cells survived after 10 min of UVA irradiation, and the percentage of survival cells decreased to 29 ± 2% after 30 min of UVA irradiation. The survival rate of HeLa cells to UVA radiation alone without any nano-TiO_2 was used as a control group (Supporting Figure S2 in the Supporting Information). About 78 ± 4% cells were alive after 10 min of exposure, whereas after 30 min of exposure, about 75 ± 2% of the cells survived. The same cytotoxicity experiments were performed using functionalized nano-TiO_2 in the presence of UVA radiation. The survival experiments of HeLa cells by APTES-TiO_2 (magenta curve) and RGDC-TiO_2 (dark yellow curve) are shown in Figure 4. Both functionalized nano-TiO_2 had a distinct cytotoxic effect on the HeLa cells. The RGDC-TiO_2 treatments resulted in a 32 ± 3 and 15 ± 2% of HeLa cells alive after 10 and 30 min of incubation, respectively. So, as a summary, RGDC-TiO_2 with the assistance of UVA radiation showed a bigger killing effect of HeLa cells than unmodified ones.

The influences of concentration of different nano-TiO_2 on the cytotoxicity of HeLa cells were also evaluated at a range from 10 to 1000 μg/mL (Figure 5). The experimental results demonstrated that for three different kinds of nano-TiO_2, the cell viability decreased monotonically as concentration of nano-TiO_2 increased. The range of TiO_2 concentrations that we chose were close to that used previously by other researches.[37] Higher concentrations of nano-TiO_2 could achieve a higher reaction rate, but cause more difficulties in separation and measurement. Based on our experiments, increasing the concentration of TiO_2 has a similar effect to increasing the incubation time.

DISCUSSION

Our genotoxicity experiments of three kinds of nano-TiO_2 to pUC19 DNA directly disclosed the interaction between different nano-TiO_2 and DNA at a single molecule level. Several important phenomena were observed. First, DNA can be damaged by unmodified nano-TiO_2 directly even without the assistance of UVA radiation. The interactions between nano-TiO_2 and plasmid DNA in the absence of UVA radiation were performed in visible light. The UV−vis absorbance curve (Supporting Figure S3 in the Supporting Information) showed that nano-TiO_2 had weak absorbance in the wavelength range of visible light that close to UVA. The band gap of TiO_2 is about 3.0 eV, which means it can only be activated by UV light.[5] However, later results showed that this band gap could be narrowed by the doping of other atoms.[27−30] In our experiments, the interactions between nano-TiO_2 and DNA or nano-TiO_2 and cells were performed in a complicated environment where many buffers and ions were included. The experimental condition that we used, together with the nanometer effects of TiO_2, might lead to the narrowing of the band gap of TiO_2. Therefore, in the experiments without UVA radiation, nano-TiO_2 might be activated partially by visible light. Second, it is clear that the damage caused by nano-TiO_2 increased if the UVA radiation was applied. The UV absorbance curve in Supporting Figure S3 in the Supporting Information showed that the biggest absorbance was at 347 nm. More ROS was produced when nano-TiO_2 was activated, which could lead to more SSB damage.

Similar to nano-TiO_2, RGDC-TiO_2 can damage DNA directly without any UVA radiation, and the amount of damage increased when UVA radiation was applied. These results agree with the unmodified nano-TiO_2, which means that the functionalization process fundamentally did not change the photocatalytic effects of nano-TiO_2. However, comparing

dx.doi.org/10.1021/jp3092804 | J. Phys. Chem. B 2013, 117, 125−131

Figure 2E−H with Figure 2A−D, RGDC-TiO_2 produced less damage than unmodified nano-TiO_2 on plasmid DNA. This implies that the coating of peptide materials on the surface of nanoparticles did block the photocatalytic effects of TiO_2 to a certain degree.

The cytotoxicities of three kinds of nano-TiO_2 to HeLa cells were measured at different incubation times and concentrations. The cytotoxicity experiments confirmed the result that nonirradiated nano-TiO_2 nanoparticles have little toxicity to the HeLa cells, which was consistent with those present in literature.[38]

However, both APTES-TiO_2 and RGDC-TiO_2 showed higher cytotoxicity to HeLa than unmodified nano-TiO_2 no matter whether UVA radiation was applied or not. This is the biggest difference from the results obtained by AFM imaging, where functionalized nano-TiO_2 showed less genotoxicity to plasmid DNA than unmodified nano-TiO_2. It is obvious that unmodified nano-TiO_2 generated more ROS than functionalized nano-TiO_2 because the surface of functionalized TiO_2 was covered by a layer of organic molecules. As a result, it is easy to understand that functionalized TiO_2 is less harmful to DNA at a molecular level, and it was also proven by our interaction experiments. However, the cytotoxicity of nanoparticles to cells is more complicated. It is not only related to the toxicity of the nanoparticle but also dependent on the probability that the nanoparticle penetrated through the cell membrane. RGDC was known to target α v β 6 integrins on the cell surface and enter the cytoplasm via receptor-mediated endocytosis,[39] which means it is easier for RGDC-TiO_2 to enter the cell. Combining these two factors together, our results showed that functionalized nano-TiO_2 has higher cytotoxicity to HeLa cells. In this case, it implies that the ability of a nanoparticle to enter the cell might be more important than its toxicity.

The genotoxicity of nano-TiO_2 to pUC19 DNA and cytotoxicity of nano-TiO_2 to HeLa cells are related and show in many ways that they follow similar rules because they adhere to similar working mechanisms. In the presence of UVA radiation, the cytotoxicities of three kinds of TiO_2 to HeLa cells increased significantly, which is similar to the results of its genotoxicity to DNA. Moreover, increasing the incubation times and the concentrations of nanoparticles will lead to higher toxicity to both DNA and cells. On the basis of our results, RGDC-TiO_2 can be a potential candidate for PDT, and one of the benefits is that UVA can work as a switch to control the activation of the therapeutic function.

CONCLUSION

In this paper, the genotoxicity and cytotoxicity of both unmodified nano-TiO_2 and RGDC functionalized nano-TiO_2 were studied in detail. The genotoxicity experiments showed that DNA was damaged by unmodified nano-TiO_2 directly even without the assistance of UVA radiation. With the assistance of UVA radiation, DNA damage increased significantly. RGDC-TiO_2 produced less damage on plasmid DNA than unmodified ones, which means the coating of peptide materials on the surface of nanoparticles blocked the photocatalytic effects of nano-TiO_2. However, different from the genotoxicity to pUC19 DNA, RGDC-functionalized nano-TiO_2 showed a higher killing effect to HeLa cells than unmodified ones with or without the assistance of UVA radiation. The contradiction between genotoxicity and cytotoxicity of RGDC-TiO_2 implied that the ability of nanoparticles to enter the cell might take an important role to its cytotoxicity. The molecular mechanisms of the cytotoxicity to HeLa cells and the genotoxicity to DNA were related but also different in certain ways. On the basis of our results, RGDC-TiO_2 can be a potential candidate for PDT, and one of the benefits is that UVA can work as a switch to control the activation of the therapeutic function.

ASSOCIATED CONTENT

Supporting Information

Control experiments of AFM imaging and MTT test associated with this paper. This material is available free of charge via the Internet at http://pubs.acs.org.

AUTHOR INFORMATION

Corresponding Author

*Tel: +86 139 139 931 09. E-mail: yj@seu.edu.cn.

Notes

The authors declare no competing financial interest.

ACKNOWLEDGMENTS

This work was supported by the National Natural Science Foundation of China (NSFC) with grant number of 21174029 to Y.J., and the project was sponsored by the Scientific Research Foundation for the Returned Overseas Chinese Scholars, State Education Ministry, to Y.J.

REFERENCES

(1) Wang, A. Z.; Langer, R.; Farokhzad, O. C. Nanoparticle Delivery of Cancer Drugs. *Annu. Rev. Med.* **2012**, *63*, 185−198.
(2) Chouikrat, R.; Seve, A.; Vanderesse, R.; Benachour, H.; Barberi-Heyob, M.; Richeter, S.; Raehm, L.; Durand, J. O.; Verelst, M.; Frochot, C. *Curr. Med. Chem.* **2012**, *19* (6), 781−792.
(3) Zhou, H.; Gan, X.; Wang, J.; Zhu, X. L.; Li, G. X. *Anal. Chem.* **2005**, *77* (18), 6102−6104.
(4) Long, T. C.; Saleh, N.; Tilton, R. D.; Lowry, G. V.; Veronesi, B. *Environ. Sci. Technol.* **2006**, *40* (14), 4346−4352.
(5) Pascual, J.; Camassel, J.; Mathieu, H. *Phys. Rev. Lett.* **1977**, *39* (23), 1490−1493.
(6) Crabtree, R. H. *Science* **1998**, *282* (5396), 2000−2001.
(7) Fujishima, A.; Honda, K. *Nature* **1972**, *238* (5358), 37.
(8) Lu, Z. X.; Zhou, L.; Zhang, Z. L.; Shi, W. L.; Xie, Z. X.; Xie, H. Y.; Pang, D. W.; Shen, P. *Langmuir* **2003**, *19* (21), 8765−8768.
(9) Ashikaga, T.; Wada, M.; Kobayashi, H.; Mori, M.; Katsumura, Y.; Fukui, H.; Kato, S.; Yamaguchi, M.; Takamatsu, T. *Mutat. Res., Genet. Toxicol. Environ. Mutagen.* **2000**, *466* (1), 1−7.
(10) Dunford, R.; Salinaro, A.; Cai, L. Z.; Serpone, N.; Horikoshi, S.; Hidaka, H.; Knowland, J. *FEBS Lett.* **1997**, *418* (1−2), 87−90.
(11) Hirakawa, K.; Mori, M.; Yoshida, M.; Oikawa, S.; Kawanishi, S. *Free Radical Res.* **2004**, *38* (5), 439−447.
(12) Steenken, S.; Jovanovic, S. V. *J. Am. Chem. Soc.* **1997**, *119* (3), 617−618.
(13) Kuchino, Y.; Mori, F.; Kasai, H.; Inoue, H.; Iwai, S.; Miura, K.; Ohtsuka, E.; Nishimura, S. *Nature* **1987**, *327* (6117), 77−79.
(14) Shibutani, S.; Takeshita, M.; Grollman, A. P. *Nature* **1991**, *349* (6308), 431−434.
(15) Hancock-Chen, T.; Scaiano, J. C. *J. Photochem. Photobiol., B* **2000**, *57* (2−3), 193−196.
(16) Muszkat, L.; Feigelson, L.; Bir, L.; Muszkat, K. A. *J. Photochem. Photobiol., B* **2001**, *60* (1), 32−36.
(17) Liu, H. T.; Ma, L. L.; Liu, J.; Zhao, J. F.; Yan, J.; Hong, F. *Toxicol. Environ. Chem.* **2010**, *92* (1), 175−186.
(18) Kolarova, H.; Tomankova, K.; Bajgar, R.; Kolar, P.; Kubinek, R. *Ultrasound Med. Biol.* **2009**, *35* (8), 1397−1404.
(19) Yamaguchi, S.; Kobayashi, H.; Narita, T.; Kanehira, K.; Sonezaki, S.; Kubota, Y.; Terasaka, S.; Iwasaki, Y. *Photochem. Photobiol.* **2010**, *86* (4), 964−971.

(20) Kubota, Y.; Shuin, T.; Kawasaki, C.; Hosaka, M.; Kitamura, H.; Cai, R.; Sakai, H.; Hashimoto, K.; Fujishima, A. *Br. J. Cancer* **1994**, *70* (6), 1107−1111.
(21) Rusling, J. F. *Biosens. Bioelectron.* **2004**, *20* (5), 1022−1028.
(22) Seo, J. W.; Chung, H.; Kim, M. Y.; Lee, J.; Choi, I. H.; Cheon, J. *Small* **2007**, *3* (5), 850−853.
(23) Wang, C.; Cao, S. Q.; Tie, X. X.; Qiu, B.; Wu, A. H.; Zheng, Z. H. *Mol. Biol. Rep.* **2011**, *38* (1), 523−530.
(24) Xu, J.; Sun, Y.; Huang, J. J.; Chen, C. M.; Liu, G. Y.; Jiang, Y.; Zhao, Y. M.; Jiang, Z. Y. *Bioelectrochemistry* **2007**, *71* (2), 217−222.
(25) Rozhkova, E. A.; Ulasov, I.; Lai, B.; Dimitrijevic, N. M.; Lesniak, M. S.; Rajh, T. *Nano Lett.* **2009**, *9* (9), 3337−3342.
(26) Sakharov, D. V.; Bunschoten, A.; van Weelden, H.; Wirtz, K. W. A. *Eur. J. Biochem.* **2003**, *270* (24), 4859−4865.
(27) Huang, K. Q.; Chen, L.; Deng, J. G.; Xiong, J. W. *J. Nanomater.* **2012**, DOI: 10.1155/2012/720491.
(28) Elfeky, S. A.; Al-Sherbini, A. S. A. *J. Nanomater.* **2011**, DOI: 10.1155/2011/570438.
(29) Zhou, M. H.; Zhang, J.; Cheng, B.; Yu, H. G. *Int. J. Photoenergy* **2012**, DOI: 10.1155/2012/532843.
(30) Umebayashi, T.; Yamaki, T.; Itoh, H.; Asai, K. *Appl. Phys. Lett.* **2002**, *81* (3), 454−456.
(31) Li, Y. X.; Wang, P.; Zhao, P.; Zhu, S. J.; Wang, X. B.; Liu, Q. H. *Ultrasonics* **2012**, *52* (4), 490−496.
(32) Xiao, S. J.; Textor, M.; Spencer, N. D.; Wieland, M.; Keller, B.; Sigrist, H. *J. Mater. Sci.: Mater. Med.* **1997**, *8* (12), 867−872.
(33) Qin, Z.; Liu, W.; Li, L.; Guo, L.; Yao, C.; Li, X. *Bioconjugate Chem.* **2011**, *22* (8), 1503−1512.
(34) Leroy, P.; Tournassat, C.; Bizi, M. *J. Colloid Interface Sci.* **2011**, *356* (2), 442−453.
(35) Jiang, Y.; Ke, C. H.; Mieczkowski, P. A.; Marszalek, P. E. *Biophys. J.* **2007**, *93* (5), 1758−1767.
(36) Jiang, Y.; Rabbi, M.; Kim, M.; Ke, C. H.; Lee, W.; Clark, R. L.; Mieczkowski, P. A.; Marszalek, P. E. *Biophys. J.* **2009**, *96* (3), 1151−1158.
(37) Xu, M. H.; Huang, N. P.; Xiao, Z. D.; Lu, Z. H. *Supramol. Sci.* **1998**, *5* (5−6), 449−451.
(38) Linnainmaa, K.; Kivipensas, P.; Vainio, H. *Toxicol. in Vitro* **1997**, *11* (4), 329.
(39) Gao, H. J.; Shi, W. D.; Freund, L. B. *Proc. Natl. Acad. Sci. U.S.A.* **2005**, *102* (27), 9469−9474.